

Molecular Modeling of the Structure and Energetics of Hydrotalcite Hydration

Jianwei Wang,* Andrey G. Kalinichev, R. James Kirkpatrick, and Xiaoqiang Hou

Department of Geology, University of Illinois at Urbana–Champaign, 1301 West Green Street, Urbana, Illinois 61801

Received June 1, 2000. Revised Manuscript Received October 17, 2000

Molecular dynamics computer simulations of Mg/Al hydrotalcite with interlayer Cl^- were performed to better understand the structure of layered double hydroxides and their hydration behavior. A set of models with variable numbers of interlayer water molecules was investigated, with the assumption of no constraints on the movements of any atoms or on the geometry of the simulation supercells. Crystallographic parameters and two components of the hydration energy were calculated. One of these components is related to the interaction of water molecules with the rest of the structure and is controlled primarily by formation of a hydrogen-bonding network in the interlayer. The other is related to expansion of the host structure itself and reflects decreasing electrostatic interactions as the c -axis expands upon swelling. The dependence of these two energy components on the degree of hydration provides useful insight into the nature of hydrotalcite swelling behavior. There are two stable hydration states with c -axis dimensions of 23.9 and 21.7 Å, corresponding to hydrotalcite with 2 water molecules per each chloride in the interlayer, and dehydrated hydrotalcite, respectively. The first state is observed experimentally under ambient atmospheric conditions. The simulations also reveal a distorted octahedral structure of the hydroxide layer similar to that of hydrocalumite, the related Ca/Al phase.

Introduction

Layered double hydroxides, LDHs, also known as mixed-metal layered hydroxides and hydrotalcite-like compounds (HTs), are an important class of readily synthesized^{1,2} natural and synthetic compounds with growing potential as anion-exchange and adsorption materials,^{3–5} carriers for drugs, antacids in medicine, electrode modifiers, catalysts, and catalyst supports.^{6,7} Many of their most important applications are due to their permanent anion-exchange and adsorption capacity, the mobility of their interlayer anions and water molecules, their large surface areas, and the stability and homogeneity of the materials formed by their thermal decomposition.⁸ They also provide useful materials for studying fundamental aspects of organic and inorganic anion intercalation.^{9–11} Their crystal structures typically consist of single sheets of metal hydrox-

ides with interlayer regions occupied by anions and water molecules. The hydroxide layers develop permanent positive charge due to isomorphic substitution. For the important Mg/Al HT compounds, this charge can be thought of as due to Al^{3+} for Mg^{2+} substitution in a brucite $\text{Mg}(\text{OH})_2$ sheet.

Understanding and predicting the properties of LDHs requires understanding of the structure of the metal hydroxide sheets and the origin of the behavior of interlayer and surface species (anions and water molecules). However, experimentally probing the interlayer and surface regions and even the detailed structure of the hydroxide sheets is difficult. For instance, X-ray diffraction has provided only limited resolution because of structural disorder and small particle size. Therefore, for most LDHs, the arrangement of interlayer water molecules and anions is not understood well, and the structure of the hydroxide layer is still under discussion.¹ Even accurate determination of the interlayer water content is difficult,¹ because H_2O molecules strongly associate with particle surfaces, and some adsorbed water is indistinguishable from interlayer water in thermal analysis. Spectroscopic methods such as multinuclear NMR are providing important new information about these issues,¹² and molecular dynamics computer simulations can also provide significant insight into the local structure and dynamical behavior of this class of compounds. In previous studies, energy minimization has been used to study LDH crystal structure and to predict the orientation of interlayer

* To whom correspondence should be addressed: e-mail jwang7@uiuc.edu.

- (1) Cavani, F.; Trifiro, F.; Vaccari, A. *Catal. Today* **1991**, *11*, 173.
- (2) Costantino, U.; Marmottini, F.; Nocchetti, M.; Vivani, R. *Eur. J. Inorg. Chem.* **1998**, 1439.
- (3) Kaneyoshi, M.; Jones, W. *Chem. Phys. Lett.* **1998**, *296*, 183.
- (4) Newman, S. P.; Jones, W. *New J. Chem.* **1998**, 105–115.
- (5) Chisem, I. C.; Jones, W. *J. Mater. Chem.* **1994**, *4* (11), 1737.
- (6) Kagunya, W.; Hassan, Z.; Janes, W. *Inorg. Chem.* **1996**, *35*, 5970.
- (7) Ulibarri, M.; Labajos, F. M.; Rives, V.; Trujillano, R.; Kagunya, W.; Janes, W. *Inorg. Chem.* **1994**, *33*, 2592.
- (8) Bellotto, M.; Rebours, B.; Clause, O.; Lynch, J.; Bazin, D.; Elkaim, E. *J. Phys. Chem.* **1996**, *100*, 8535.
- (9) Kanezaki, E.; Kinugawa, K.; Ishikawa, Y. *Chem. Phys. Lett.* **1994**, *226*, 325.
- (10) Kuk, W.; Huh, Y. *J. Mater. Chem.* **1997**, *7* (9), 1933.
- (11) Serwicka, E. M.; Nowak, P.; Gahranowski, K.; Jones, W.; Kooli, F. *J. Mater. Chem.* **1997**, *7* (9), 1937.

- (12) Hou, X.; Kirkpatrick, R. J.; Yu, P.; Moore, D.; Kim, Y. *Am. Mineral.* **2000**, *85*, 133.

anions,¹³ and molecular dynamics (MD) has been used to study LDHs with intercalated organic molecules.^{14–16} The simulations reproduced well the hydration profile (*c*-axis expansion) related to the orientation of the organic molecules. We have recently used molecular modeling methods to study the structure and dynamics of the interlayer and surface species of hydrocalumite (also known as Friedel's salt, $[\text{Ca}_2\text{Al}(\text{OH})_6]\text{Cl}\cdot 2\text{H}_2\text{O}$), which is structurally one of the best understood LDHs and similar to the Mg/Al compounds.¹⁷ Monte Carlo and molecular dynamics methods have also been used to study the properties of clay minerals,^{18,19} including their interlayer structure and their hydration and related swelling.^{20–26} In many of these simulations, atoms of the main oxide layers are often treated as fixed in a rigid lattice, except for the degrees of freedom associated with swelling and lateral displacements of the lattice as a whole. This simplified approach is computationally efficient and provides useful structural information. However, it also has inherent and substantial limitations for the dynamic modeling of surface and interlayer species. Due to the immobility of the lattice atoms, there is no exchange of momentum and energy between the atoms of the main layers and the interlayer/surface species. Thus, in these models the imposed momentum and energy conservation laws a priori prevent accurate representation of the dynamics of such phenomena as hydrogen bonding, adsorption, and surface complexation.

Here we present a molecular dynamics study of the structure and hydration behavior of Mg/Al hydrotalcite with chloride as the interlayer anion, $[\text{Mg}_2\text{Al}(\text{OH})_6]\text{Cl}\cdot N_{\text{w}}\text{H}_2\text{O}$. All atoms in our hydrotalcite models were considered completely movable, and the simulation techniques are similar to those of Kalinichev et al.¹⁷ The results provide important insight into the structure of the main hydroxide layer, the nature of the most stable hydration states, the structural expansion with increasing water content (the swelling profile), and the important components of the hydration energy.

Structural Models and Simulation Details

The structural models used here are based on a crystal structure of Mg/Al hydrotalcite obtained by a refinement of

powder X-ray diffraction data from Rietveld methods.²⁷ This structure is broadly similar to that of hydrocalumite (Friedel's salt), for which the structure is well-known from single-crystal X-ray refinements.²⁸ However, the structure of hydrotalcite is not as well constrained because it is based on powder X-ray data. Our simulations show that the structure of Mg/Al hydrotalcite is more similar to that of hydrocalumite than previously thought.

For two common polytypes of hydrotalcite-like phases (3R and 2H),²⁷ the local structural environments are the same, although the long-range ordering of the hydroxide layers is different. The Mg/Al hydrotalcite structure has been refined in a rhombohedral unit cell with the space group $R\bar{3}m$,^{27,29} and we have assumed $R\bar{3}m$ symmetry for the initial configuration of the primary layers in our models.

We have also assumed complete Mg/Al ordering in the hydroxide layers. Long-range cation ordering in LDHs has been difficult to observe by powder X-ray diffraction, except for the Ca/Al, Li/Al, and Mg/Ga phases.^{27,28} However, evidence for significant short-range cation ordering in other LDHs comes from X-ray absorption spectroscopy (XAS) and nanoscale imaging of molecular sorption onto crystal surfaces.^{29–31} XAS shows the absence of Fe–Fe neighbors in Mg/Fe hydrotalcite, suggesting domains of cation ordering with dimensions of the order of a few nanometers. Similar short-range ordering is expected in Mg/Al hydrotalcite.²⁹ In support of this conclusion, AFM and STM images show ordered two-dimensional lattices of organic and inorganic anions adsorbed on the [001] surfaces of Mg/Al hydrotalcite crystals.^{30,31} Thus, in our models each Al–O octahedron has six nearest-neighbor Mg–O polyhedra, and each Mg–O polyhedron has three nearest-neighbor Mg–O polyhedra and three nearest-neighbor Al–O octahedra.

The final simulated supercell contained a total of 18 crystallographic unit cells, $6 \times 3 \times 1$ in the *a*-, *b*-, and *c*-directions, respectively. Thus, every octahedral layer had 12 Mg atoms, 6 Al atoms, and 36 OH groups. To study the expansion behavior, each supercell contained three interlayers, consisting of 6 Cl^- ions and from 0 to 40 water molecules (Figure 1). In a given simulation each of the three interlayers had the same $\text{H}_2\text{O}/\text{Cl}$ ratio, N_{w} , but a different initial configuration. In the previously published X-ray structure refinement of Mg/Al hydrotalcite, the positions of the interlayer anions and water molecules were preassigned at the center of the interlayer space along the *c*-axis.²⁷ In the simulations, however, we initially allowed the interlayer anions and water molecules to occupy all available interlayer space in order to minimize the possibility of the system being locked in a local energy minimum of the structure. Thus, there were no initial positional correlations among H_2O and Cl^- in the interlayers.

Except for the periodic boundary conditions imposed on the simulation supercell,³² there were no additional symmetry constraints. The structure was treated as triclinic (*P1* symmetry) and all cell parameters, *a*, *b*, *c*, α , β , and γ , were considered independent variables during our isothermal–isobaric MD simulations. Each atom in the system had an assigned partial charge, and the total potential energy of the simulated system consisted of a Coulombic term representing the sum of all electrostatic interactions between partial atomic charges and a Lennard-Jones (12–6) term modeling the short-range van der Waals interactions. The force field used in the simulations was modified from the augmented ionic consistent valence (CVFF_aug) force field.³³ Instead of placing full formal

(13) Fogg, A. M.; Rohl, A. L.; Parkinson, G. M.; O'Hare, D. *Chem. Mater.* **1999**, *11*, 1194.

(14) Williams, S. J.; Coveney, P. V.; Jones, W. *Mol. Simul.* **1999**, *21*, 183.

(15) Aicken, A. M.; Bell, I. S.; Coveney, P. V.; Jones, W. *Adv. Mater.* **1997**, *9*, 496.

(16) Newman, S. P.; Williams, S. J.; Coveney, P. V.; Jones, W. *J. Phys. Chem. B* **1998**, *102*, 6710.

(17) Kalinichev, A. G.; Kirkpatrick, R. J.; Cygan, R. T. *Am. Mineral.* **2000**, *85*, 1046.

(18) Skipper, N. T.; Chang, F. C.; Sposito, G. *Clays Clay Miner.* **1995**, *43*, 285.

(19) Teppen, B. J.; Rasmussen, K.; Bertsch, P. M.; Miller, D. M.; Schafer, L. *J. Phys. Chem. B* **1997**, *101*, 1579.

(20) Hartzell, C. J.; Cygan, R. T.; Nagy, K. L. *J. Phys. Chem. A* **1998**, *102*, 6722.

(21) Karaborni, S.; Smit, B.; Heidug, W.; Urai, J.; Oort, E. V. *Science* **1996**, *217*, 1102.

(22) De Siqueira, A. V. C.; Skipper, N. T.; Coveney, P. V.; Boek, E. S. *Mol. Phys.* **1997**, *92*, 1.

(23) Greathouse, J.; Sposito, G. *J. Phys. Chem. B* **1998**, *102*, 2406.

(24) Smith, D. E. *Langmuir* **1998**, *14*, 5959.

(25) Chang, F. C.; Skipper, N. T.; Sposito, G. *Langmuir* **1998**, *14*, 1201.

(26) Boek, E. S.; Coveney, P. V.; Skipper, N. T. *J. Am. Chem. Soc.* **1995**, *117*, 12608.

(27) Bellotto, M.; Rebours, B.; Clause, O.; Lynch, J.; Bazin, D.; Elkaim, E. *J. Phys. Chem.* **1996**, *100*, 8527.

(28) Terzis, A.; Filippakis, S.; Kuzel, H. J.; Burzlaff, H. Z. *Kristallogr.* **1987**, *181*, 29.

(29) Vucelic, M.; Jones, W.; Moggridge, G. D. *Clays Clay Miner.* **1997**, *45*, 803.

(30) Cai, H.; Hillier, A. C.; Franklin, K. R.; Nunn, C. C.; Ward, M. D. *Science* **1994**, *266*, 1551.

(31) Yao, K.; Taniguchi, M.; Nakata, M.; Takahashi, M.; Yamagishi, A. *Langmuir* **1998**, *14*, 2410.

(32) Allen, M. P.; Tildesley, D. J. *Computer Simulation of Liquids*; Oxford University Press: New York, 1987; p 385.

(33) Molecular Simulations, Inc. Cerius²-4.0 User Guide, 1999.

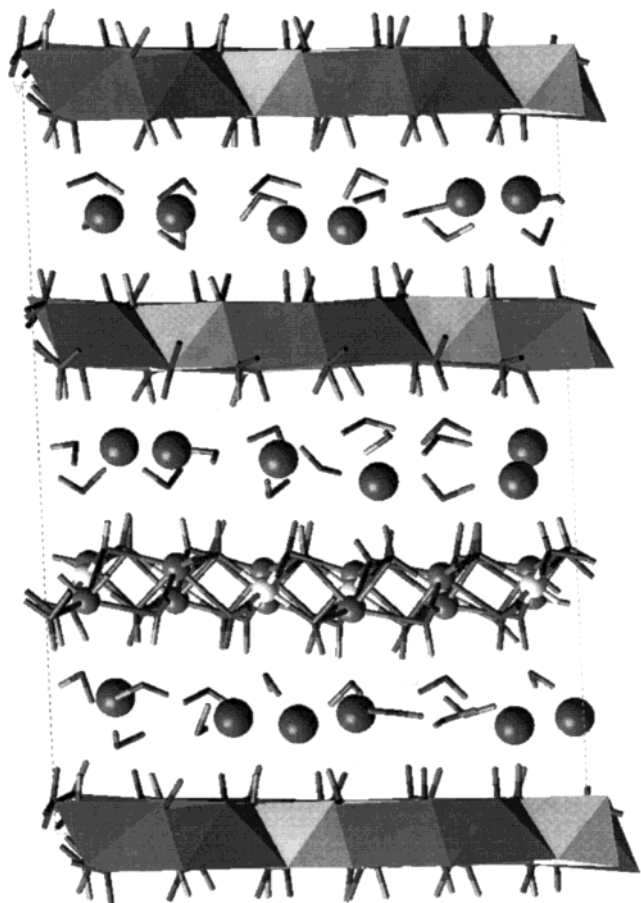


Figure 1. Simulation supercell of hydrotalcite, consisting of $6 \times 3 \times 1$ crystallographic unit cells. There are three octahedral layers and three interlayers. Dark gray octahedrons and small dark gray balls are Mg atoms, white octahedrons and small white balls are Al atoms, the gray sticks are OH groups, white large balls are Cl^- , and water molecules are represented by bent cylinders. Half of the Mg atoms are shifted up from the middle of the hydroxide layer and the other half are shifted down from the middle. Water molecules and anions are disordered. The structure represents an equilibrium snapshot of a molecular dynamics simulation.

charges on the metal ions in the hydroxide layer, we performed preliminary quantum-mechanical calculations to determine appropriate partial charges. The specific details of the force field parametrization are reported elsewhere.^{17,34} For water, the flexible version³⁵ of the simple point charge (SPC) interaction potential³⁶ was used. Lennard-Jones terms centered on the O atoms were assumed equivalent for both H_2O molecules and OH-group oxygens of the hydroxide layers, while those centered on the H atoms were ignored.

For the potential energy calculations, a “spline cutoff” method was used to calculate nonbonding van der Waals interactions, and Ewald summation was used to calculate long-range Coulombic interactions.³³ Energy minimization was applied to every model. These optimized models were then used as starting configurations for NPT-ensemble MD simulations performed at 1 bar and 300 K by use of the Parrinello–Rahman³⁷ isothermal–isobaric molecular dynamics algorithm.

(34) Cygan, R. T.; Liang, J.; Kalinichev, A. G. Manuscript in preparation.

(35) Teleman, O.; Jönsson, B.; Engström, S. *Mol. Phys.* **1987**, *60*, 193.

(36) Berendsen, H. J. C.; Postma, J. P. M.; van Gunsteren, W. F.; Hermans, J. Interaction models for water in relation to protein hydration. In *Intermolecular Forces*, Pullman, B., Ed.; Riedel: Dordrecht, The Netherlands, 1981; p 331.

(37) Parrinello, M.; Rahman, A. *J. Appl. Phys.* **1981**, *52*, 7182.

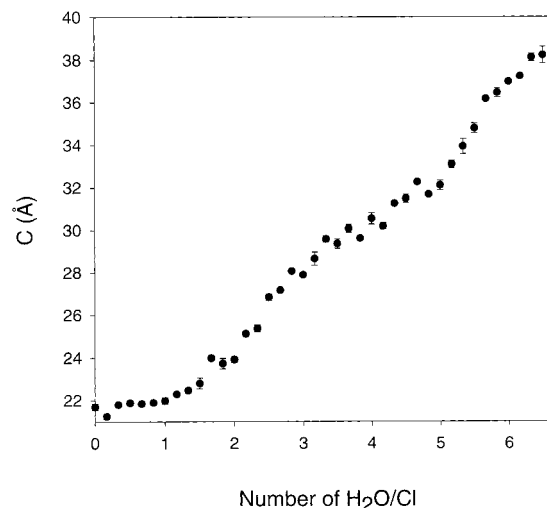


Figure 2. c -Axis dimension swelling upon hydration of hydrotalcite. The values and error bars are statistical averages and standard deviations calculated from 5 ps equilibrium MD simulations. In many cases the standard deviations are less than the symbol size.

The MD time step was 0.001 ps, and dynamic trajectories were recorded every 0.004 ps. Initially, 100 ps long MD simulations were performed for several representative systems. The results showed that equilibrium values for the crystallographic parameters and system potential energy were achieved within less than 20 ps. Therefore, for most of the systems, 25 ps MD runs were performed with only the last 5 ps of each dynamic trajectory used for the statistical analysis. This provided acceptable statistics for the hydration profile and potential energy calculations for a total of 41 systems corresponding to different hydration states with N_w varying from 0 to 6.67.

Results and Discussion

Hydrotalcite Crystal Structure. The computed crystallographic dimensions and configurations of the hydroxide layers do not vary significantly with N_w . The average a - and b -axis lengths are $3.196 (\pm 0.008)$ and $3.197 (\pm 0.009)$ Å, the γ angle is $120^\circ (\pm 0.5^\circ)$, and the α and β angles fluctuate around 90° . These values compare well with the available experimental data: $a = b = 3.046$ Å, $\alpha = \beta = 90^\circ$, and $\gamma = 120^\circ$.²⁷ The computed c -axis dimension increases with increasing N_w (Figure 2), but there are three important ranges where it is almost independent of N_w . For $N_w < 1$, the c -axis lengths are about 21.7 Å. Near $N_w \approx 2$ the Cl^- and H_2O form a complete single layer in each interlayer region (similar to the interlayer of hydrocalumite²⁸ but significantly more disordered) and the computed c -axis dimension is 23.9 Å. This is in excellent agreement with the value of 23.6 Å obtained from X-ray diffraction for hydrated Cl^- -Mg/Al hydrotalcite under ambient conditions.^{38,39} Near $N_w \approx 5$ a complete second layer of water molecules is formed in each interlayer space, and our simulations give a c -axis dimension of 31.8 Å. Since Mg/Al Cl-hydrotalcite does not expand beyond 23.9 Å at any relative humidity and atmospheric pressure, this hydration state has not been observed experimentally.¹

The Al and Mg polyhedra in the hydroxide layer are quite different, in agreement with the known structure

(38) Boclair, J. W.; Braterman, P. S.; Brister, B. D.; Yarberry, F. *Chem. Mater.* **1999**, *11*, 2199.

(39) Titulaer, M. K.; Talsma, H.; Jansen, B. H.; Geus, J. W. *Clay Miner.* **1996**, *31*, 263.

of the Ca/Al LDH hydrocalumite²⁸ but in contrast to the structure refinement of Mg/Al hydrotalcite obtained from powder X-ray diffraction data from Rietveld methods.²⁷ The resolution in the latter structure refinement is not adequate to distinguish separate Mg and Al sites, and given the similarity between the observed²⁸ and simulated¹⁷ structures of Ca/Al hydrocalumite and presently simulated structure of Mg/Al hydrotalcite, it is likely that this simulated structure more accurately represents the actual local structure of Mg/Al hydrotalcite.

The Al-polyhedra in the hydroxide layers are quite regular Al(OH)₆ octahedra with Al–O distances of about 1.9 Å. The O–O distances of the unshared octahedral edges are about 2.7 Å. The Al atoms are located in the middle of hydroxide layers along the *c*-axis. The Mg-polyhedra are distorted Mg(OH)₆ octahedra, and additionally most have either an interlayer H₂O molecule or a Cl[−] ion coordinated to the Mg (at distances of about 2.4 and 3.0 Å, respectively), forming a 7-coordinate site. The Mg atoms are displaced about 0.5 Å from the middle of hydroxide layers along the *c*-direction, with half of them shifted up and half shifted down (Figure 1). The Mg–O distances are about 2.32 Å, and the O–O distances of the unshared octahedral edges are about 3.0 and 3.9 Å. The number-weighted mean value of the Mg–O and Al–O distances is 2.18 Å and the number-weighted mean unshared O–O distance is 3.20 Å, compared to the experimental values of 2.013 and 3.05 Å, respectively.²⁷

The unusual 7-coordinated Mg-polyhedron and the displacement of Mg atoms from the middle of hydroxide layers are in good agreement with the behavior of Ca atoms in hydrocalumite observed in both X-ray refinements²⁸ and computed structures.¹⁷ In hydrocalumite, Ca atoms are displaced about 0.6 Å from the middle of hydroxide layers and have 7-fold coordination by 6 OH groups and one water molecule.^{17,28} Thus, our results for the smaller Mg atoms in Mg/Al hydrotalcite suggest that many LDHs may have structures similar to that of hydrocalumite. We have previously related this structure and the attendant libration of the water molecules to the presence of experimentally observed dynamical order–disorder phase transitions in both hydrocalumite and Mg/Al hydrotalcite.^{40,17}

The structure and cation ordering in the hydroxide layers strongly affect the structure and anion ordering in the interlayer of LDHs. There are two kinds of sites on the hydroxide layer of LDHs that have a net effective positive charge and can, thus, attract either negatively charged Cl[−] anions or H₂O molecules, which bear a negative atomic partial charge on their O atoms. One of these sites, as discussed above, is associated with the Mg (or Ca of hydrocalumite) due to its shift toward the interlayer. In the interlayer of fully ordered hydrocalumite,²⁸ all sites of this kind are occupied by water molecules, which are displaced ≈0.8 Å from the central plane of the interlayer by the electrostatic forces.¹⁷ This effectively creates two sublayers of H₂O molecules associated with Ca or Mg cations in the “upper” and “lower” hydroxide layers sandwiching an interlayer.

The second kind of a positively charged attractive site on the hydroxide layer is formed by the protons of the hydroxyl groups. In the structure of hydrocalumite,²⁸ all sites of this kind are occupied by Cl[−] anions, each of them being octahedrally coordinated by three OH groups from the “upper” and three OH groups from the “lower” hydroxide layers. This symmetric hydrogen-bonding arrangement keeps Cl[−] ions virtually immobile in the middle of the interlayer space even at high temperatures.¹⁷ In the classification of layer stacking in hydrotalcite-like phases developed by Bookin and Drits,⁴¹ both kinds belong to the O-type of interlayer sites, which have an octahedral configuration. From the stoichiometry of the compounds and the diameters of the interlayer species (≈3 Å for H₂O and ≈4 Å for Cl[−]) it is clear that only 6 Cl[−] ions and 12 H₂O molecules (distributed between two sublayers) can occupy the interlayer space without expanding it.

The same two kinds of attractive sites for interlayer species occur on the hydroxide layers of Mg/Al hydrotalcite. They also both belong to the O-type of interlayer sites. However, due to the stacking differences of the hydroxide layers between Ca/Al hydrocalumite^{17,28} and our Mg/Al hydrotalcite models, the observed interlayer structures and Cl[−]/H₂O ordering are also different, and hydrotalcite is much more disorderd. Mg sites tend to be occupied by Cl[−] ions but can also be occupied by H₂O molecules, especially at higher interlayer water contents. This again creates two sublayers of water molecules in the interlayer (see Figure 1). The positional disorder of the interlayer water molecules results in the formation of a much less regular network of hydrogen bonds in the interlayer of Mg/Al hydrotalcite, as opposed to Ca/Al hydrocalumite.¹⁷ Computer simulations of the effects of interlayer ordering and varying water content on the dynamic properties of the interlayer species are currently in progress.

Energetics of Hydrotalcite Hydration. There are several useful parameters that can be obtained from the variation of the computed potential energy with N_w , and we use these functions below to understand the hydration behavior. We use the same definition of the hydration energy, $\Delta U_H(N)$, that was introduced earlier in studies of clay mineral swelling:^{24,26}

$$\Delta U_H(N) = \frac{\langle U(N) \rangle - \langle U(0) \rangle}{N} \quad (1)$$

where $\langle U(N) \rangle$ is the average potential energy of an equilibrium system with N water molecules in the interlayer and $\langle U(0) \rangle$ is the average potential energy of equilibrated (fully collapsed) dry hydrotalcite as a reference hydration state.

As defined above, the hydration energy includes not only the potential energy of interlayer water but also the effects on the potential energy of the changing interactions of the hydroxide layers with themselves, the hydroxide layers and the chloride ions, and the chlorides with themselves. We can consider the hydration process to consist of two steps. First, energy is necessarily used to expand an equilibrium structure to create additional interlayer space for more water molecules. Second, the energy lost in the first step can be

(40) Kirkpatrick, R. J.; Yu, P.; Hou, X.; Kim, Y. *Am. Mineral.* **1999**, *84*, 1186.

(41) Bookin, A. S.; Drits, V. A. *Clays Clay Miner.* **1993**, *41*, 551.

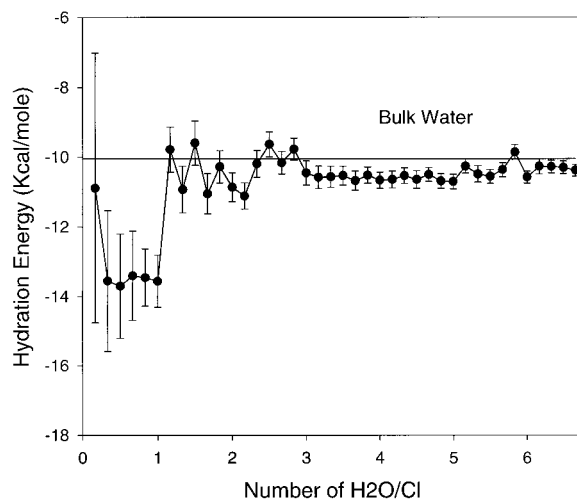


Figure 3. Hydration energy of hydrotalcite calculated according to eq 1. In this calculation, $\langle U(N) \rangle$ is the statistical average with a standard deviation, and $\langle U(0) \rangle$ is the constant equilibrium energy of a completely dehydrated hydrotalcite structure taken as a reference.

compensated by energy gain due mainly to the presence of additional water molecules, rearrangement of interlayer species, optimization of the re-formed hydrogen-bonding network, and equilibration of the system in a new hydration state. Thus, to better understand the nature of hydrotalcite hydration behavior, we separate the hydration energy (eq 1) into two components. The interlayer water potential energy is defined as

$$\Delta U_{\text{H}_2\text{O}}(N) = \frac{\langle U(N) \rangle - \langle U(N, \text{without H}_2\text{O}) \rangle}{N} \quad (2)$$

where $\langle U(N, \text{without H}_2\text{O}) \rangle$ is the average potential energy of the hypothetical systems obtained in the simulations by removing all N water molecules from all interlayers of a system corresponding to a given hydration state, but keeping the rest of system intact, including the c -axis spacing.

The water-free potential energy difference is defined as

$$\Delta U_{\text{HT}}(N) = \langle U(N, \text{without H}_2\text{O}) \rangle - \langle U(0) \rangle \quad (3)$$

and represents the energy difference between two states of the water-free hydrotalcite structure: a nonequilibrium state obtained by simply removing all H_2O molecules from a system in a certain hydration state, and an equilibrium (collapsed) state of dry hydrotalcite. The latter is obtained from the former by application of energy minimization and relaxation procedures.

Hydration Energy. The hydration energy $\Delta U_{\text{H}}(N)$ (Figure 3) is the average potential energy of the system per mole of water, with dry hydrotalcite taken as the reference state. There are several important ranges of N_{w} for this function. For $N_{\text{w}} < 1$, the hydration energy is quite negative, indicating a strong tendency for water molecules to enter the dry structure. At N_{w} near 2, there is a clear minimum of the hydration energy that corresponds to the region of N_{w} -independent c -axis dimensions (Figure 2) and to the normal equilibrium state of Mg/Al hydrotalcite at ambient conditions. As the number of interlayer water molecules increases

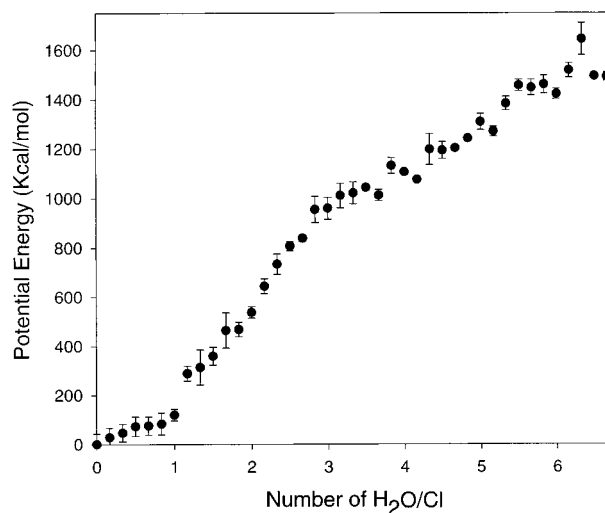
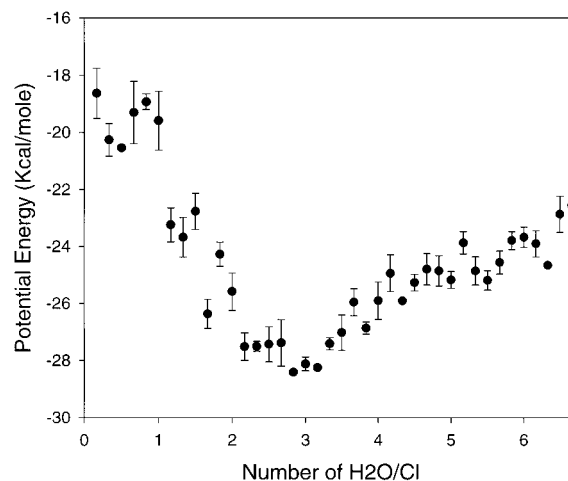


Figure 4. (Top panel) Interlayer water potential energy. (Bottom panel) Water-free potential energy difference. Error bars are calculated from the maximum and minimum values of the system potential energy during equilibrium 5 ps MD simulations.

further, the hydration energy gradually approaches values characteristic of bulk SPC water (about -10.0 kcal/mol). Because the system $P\Delta V$ term is relatively small at ambient conditions (≈ 0.01 kcal/mol), the hydration energy virtually coincides with the system hydration enthalpy. Thus, there are two enthalpic stable states of the hydrotalcite hydration, at $N_{\text{w}} \leq 1$ and at $N_{\text{w}} = 2$. The slope of the hydration energy function can be considered as the enthalpic driving force for hydration and dehydration of the material. Although the hydration behavior could be represented by other thermodynamic functions,²⁴ the positions of the minima would still be the same.

Two Components of the Hydration Energy. The interlayer water potential energy, $\Delta U_{\text{H}_2\text{O}}(N)$ (Figure 4, top panel) and the water-free potential energy difference, $\Delta U_{\text{HT}}(N)$ (Figure 4, bottom panel), as defined by eqs 2 and 3, allow the effects due to the water molecules and the sum of all other interactions to be evaluated separately. $\Delta U_{\text{H}_2\text{O}}(N)$ has negative values, indicating an energetically favorable contribution to the hydration due to the addition of water molecules. In contrast, $\Delta U_{\text{HT}}(N)$ has positive values, indicating an unfavorable contribution to the hydration energy brought about by the expansion of the water-free hydrotalcite framework.

The two components make different contributions to the hydration energy at different stages of hydration. In the range $0 < N_w < 1$, $\Delta U_{\text{H}_2\text{O}}(N)$ is nearly constant, and $\Delta U_{\text{HT}}(N)$ is small and increases only slightly. Thus, the net hydration energy is quite negative and each extra water molecule makes nearly the same contribution to the hydration energy. We interpret this result to indicate that each water molecule experiences nearly the same local structural and energetic environment and that there are not enough water molecules present in the interlayer space to develop a well-interconnected hydrogen-bonding network among themselves and the Cl^- ions and the OH groups of the adjacent octahedral sheets. Thus, these first H_2O molecules simply fill vacant positions in the interlayer without changing the c -axis dimension and create only a few hydrogen bonds with the neighboring hydroxides and chlorides. In this range no energy is lost to the expansion, because expansion is not necessary to accommodate the few H_2O molecules in the almost empty interlayer gallery space formed by the larger chloride ions pillaring the two adjacent octahedral sheets. The net effect is that the hydration energy is quite negative and nearly constant in this range (Figure 3).

In the range $1 < N_w < 3$, $\Delta U_{\text{HT}}(N)$ increases significantly, whereas $\Delta U_{\text{H}_2\text{O}}(N)$ decreases significantly in the range $1 < N_w < 2$ and then remains nearly constant for $2 < N_w < 3$. The net effect is that there is a minimum in the hydration energy at $N_w \approx 2$, where the interlayer species form a full layer. The decreasing $\Delta U_{\text{H}_2\text{O}}(N)$ indicates that each extra water molecule makes a progressively increasing contribution to the hydration energy by creating more hydrogen bonds and eventually forming a well-developed H-bonding network as the number of water molecules approaches $N_w = 2$. This hydrogen-bonding network, although disordered, is quite comparable to that of hydrocalumite.^{17,28}

For $N_w > 3$, both $\Delta U_{\text{H}_2\text{O}}(N)$ and $\Delta U_{\text{HT}}(N)$ increase progressively, although $\Delta U_{\text{H}_2\text{O}}(N)$ appears to have a local minimum or flattening near $N_w = 5$. At $N_w = 5$, a complete second layer of interlayer species is fully developed. A full layer of interlayer species in our supercell requires 18 particles (12 H_2O and 6 Cl^- at $N_w = 2$), and a full second layer requires additional 18

particles (a total of 30 H_2O and 6 Cl^- at $N_w = 5$). This packing mechanism is consistent with earlier work.⁴²

The computed hydration energies suggest that almost dry Mg/Al hydrotalcite with just a few interlayer water molecules and hydrotalcite with two water molecules per formula unit should be stable, and indeed the second composition, $[\text{Mg}_2\text{Al}(\text{OH})_6]\text{Cl}\cdot 2\text{H}_2\text{O}$, is readily observed in experiments.^{38,39} Large negative values of the hydration energy at low N_w ratios suggest a strong tendency of dry hydrotalcite to sorb water even at low relative humidities. At the same time, the apparent shallow minimum of the interlayer water potential near $N_w = 5$ (two completed layers of interlayer species) suggests that this situation might be stable at elevated water pressures, although it has not been observed under ambient conditions.

It appears that the formation of well-developed hydrogen-bonding networks associated with completely packed interlayers leads to energetically stable hydration states of hydrotalcite. The development of hydrogen bonding also explains the large decrease in the interlayer water potential energy at $N_w = 1$. At this composition, there are 12 particles per interlayer (6 H_2O and 6 Cl^-), and water molecules can fill only half of the available water sites of a full interlayer. As more water molecules are added beyond this ratio, they are able to form local structural and energetic environments similar to those in the full layer, thus effectively reducing potential energy per water molecule. For the total hydration energy, however, this effect is counteracted by interlayer expansion.

Acknowledgment. This research was supported by NSF (Grants EAR 95-26317 and EAR 97-05746) and partly by National Computational Science Alliance (Grant EAR 990003N) and utilized NCSA SGI/CRAY Origin 2000 computers. The computations were performed with the Cerius²-4.0 software package from Molecular Simulations Inc. Useful discussions with R. T. Cygan and P. Yu concerning the force field parametrization and the structures of LDHs are most gratefully acknowledged.

CM000441H

(42) Miyata, S. *Clays Clay Miner.* **1975**, *23* 369.